

Recent Results of NICT Caesium Atomic Fountains

Motohiro Kumagai, Hiroyuki Ito, Masatoshi Kajita, Mizuhiko Hosokawa
National Institute of Information and Communications Technology (NICT)
Tokyo, Japan
mkumagai@nict.go.jp

Abstract— National Institute of Information and Communications Technology (NICT) has developed Cs atomic fountain frequency standards aiming at contributing to improve the accuracy of International Atomic Time (TAI) and Japan Standard Time. They are called NICT-CsF1 and NICT-CsF2. The accuracy evaluation of CsF1 has been completed and a Type B uncertainty of 1.9×10^{-15} has been achieved. NICT-CsF2 is under development.

I. INTRODUCTION

NICT has developed the atomic fountain type primary frequency standards for the purpose of contribution to the accuracy of TAI in the level of 10^{-15} and improving Japan Standard Time (JST). JST has been responsibly maintained for a long time by NICT [1]. Recently, we have developed a new atomic fountain frequency standard named “NICT-CsF1” [2, 3]. CsF1 is designed to be compact for stable operation with making the most use of our experience with a proto-type [4]. In this paper, we describe the structure of our first operational fountain CsF1 and the evaluation of its frequency shifts and the related uncertainties. The validity of CsF1 checked by comparing with TAI or other institute’s frequency standard is also shown here. As for CsF1, we are preparing for a more complete and detailed paper, which will be published somewhere. And, we have been developing the second caesium atomic fountain NICT-CsF2 to confirm the accuracy evaluations by comparing two atomic fountains. We preview the structure of CsF2 briefly.

II. SYSTEM DESCRIPTION OF NICT-CSF1

NICT-CsF1 consists of three parts; a laser cooling region, a microwave interaction region and a detection region. The detection region is located between the laser cooling region and the microwave interaction region. A selection cavity, which pre-selects $m_F = 0$ atoms, is installed just above the laser cooling region (about 8cm above the loading point). The microwave interaction region has a C-field coil and a cylindrical microwave cavity. The cavity has a TE_{011} resonance mode, whose loaded quality factor is about 18000. The microwave interaction region is surrounded by three-layers magnetic shield, which produce the shielding of order 10^3 . The detection chamber has three laser interaction areas where the falling atoms are irradiated with the detection beams. Two sets of spherical mirrors (diameter of about 20 mm) are mounted at the highest and the lowest ports to increase fluorescence collection efficiency. The fluorescence light collected by each mirrors is focused on a photo detector via a light pipe. In all regions, ultra high vacuum ($< 2 \times 10^{-7}$

Pa) has been achieved by using two ion pumps and two non-evaporable getter (NEG) pumps, which are effective to hydrogen.

Two extended-cavity diode lasers are used as master lasers. Both lasers are stabilized to Cs D_2 absorption by modulation transfer spectroscopy technique. Two 150mW laser diodes are injection-locked by the highly stabilized ECDL to amplify the laser power for the laser cooling. The frequency and the power of each laser beam are controlled with acousto-optics modulator. Each laser beam is delivered to the vacuum chamber through a polarization maintaining fiber. The diameters of the laser beams, which are circular-polarized, are 12mm for the vertical beams and 25mm for the horizontal beams with the power density of at least 10mW/cm^2 . A portion of the output is used for detection. The other ECDL is used as a repumper at the laser cooling and the detection.

As the source of 9.192GHz microwave interrogation, we use a synthesizer of Spectra Dynamics Incorporation (SDI CS-1) [5]. All VCXOs and DDS are phase-locked to the 5MHz of the hydrogen maser, which is linked to UTC(NICT). The spurs and harmonics are more than 60 dB below the carrier. The output of the synthesizer is divided for two coupling of the microwave cavity, and the relation of two microwave feedings is adjustable with a phase-shifter.

III. FOUNTAIN OPERATION

NICT-CsF1 operates with the following steps; capture of atoms by the MOT, launching upward and post-cooling, state-selection, Ramsey interaction (two microwave interactions) and detection. Including the communication times with the instruments, the operation cycle lasts about 1.5 sec.

Cs atoms are captured in a magneto-optical trap (MOT), and then cooled in optical molasses. The atoms are launched upward by (0,0,1) moving molasses. The launched atoms are post-cooled to about 2 μK by polarization gradient cooling. All the laser beams are blocked by mechanical shutters after the launching. In the selection cavity, the $m_F = 0$ components of the launched atoms ($F = 4$) are pumped to the ($F = 3$, $m_F = 0$) state by the π -pulse microwave excitation. The others in the $F = 4$ state are blasted away by the radiation pressure of the downward beams. The ($F = 3$, $m_F = 0$) atoms continue the ballistic flight into the microwave cavity. Two $\pi/2$ -pulse microwave interactions at going upward and downward move

the atom from the ($F=3$, $m_F=0$) state to the ($F=4$, $m_F=0$) state with following the transition probability. To avoid the noise due to cycle-to-cycle fluctuation of the number of the launched atoms, the signal is normalized by measuring both the number of the $F=4$ atoms and the number of the $F=3$ atoms separately at the detection zone.

The interrogated microwave frequency is locked to the narrow Ramsey resonance by the frequency modulation locking method, in which the microwave is toggled between $f_0 - \Delta\nu/2$ and $f_0 + \Delta\nu/2$, where f_0 is the microwave central frequency, and $\Delta\nu$ is the linewidth of the Ramsey fringe, at each cycle. f_0 is controlled to make the signal intensities at the two frequencies equal by steering the output frequency of the DDS in the synthesizer. The mean frequency of two toggled frequencies is recorded as the frequency realized by NICT-CsF1 against the local oscillator (LO). At present, we use the hydrogen maser as the LO. So far, the frequency stability of $4 \times 10^{-13} / \tau^{1/2}$ has been achieved. In NICT-CsF1, the reduction of the number of the atoms, which generate the Ramsey signal, does not significantly degrade the stability. It suggests that the short-term stability of NICT-CsF1 is limited by the phase noise of the LO and the Dick effect.

IV. SYSTEMATIC FREQUENCY SHIFTS

The systematic shifts identified for NICT-CsF1 are evaluated with their uncertainties theoretically and experimentally. The results are summarized in Table 1.

A. Second-order Zeeman Shift

The correction for the second-order Zeeman shift is calculated by monitoring the ($F=4$, $m_F=1$) – ($F=3$, $m_F=1$) transition with linear dependence on the magnetic field B . This transition is also used to check the homogeneity of the magnetic field along the atomic trajectory. The C-field of

NICT-CsF1 is typically 125 nT and the variance is 0.4 nT. The offset due to the magnetic inhomogeneity is of the order of 10^{-19} , which is negligible. The uncertainty of the second-order Zeeman shift is dominated by the temporal instability of B . In NICT-CsF1, the temporal variation of the monitored transition frequency is less than 0.5 Hz, leading to an uncertainty of less than 1×10^{-16} .

B. Collision Shift

The frequency shift due to collision between cold atoms is evaluated by extrapolating to zero density when amounts of the shift have a linear relation with the atomic number densities. To vary the atomic density without changing the atomic cloud size, only the intensity of the microwave fed to the selection cavity is controlled. All data are obtained by operating alternatively at two points of the atomic densities, each for 48 hours to avoid the instability of the reference. The two points are chosen randomly from $N = 0.3$ to 2.2. N is the signal intensity relative to that at the regular operation ($N=1$) in the arbitrary unit, indicating the atomic number density in the cloud. The result of the atomic number mapping is shown in Fig.1. The frequency shift linearly depends on N over a range from $N = 0.3$ to 2.2 has been confirmed. The coefficient of the fractional frequency shift to the atomic number density is determined by averaging the results, which are obtained from each alternative operation. The coefficient is calculated as $\alpha = -8.2$ with a standard deviation of 1.7. From this result, we estimate the frequency shift due to the cold collisions with 20% uncertainty. During the measurement campaign, however, we do not use this historical slope coefficient for the zero-density extrapolation. NICT-CsF1 is operated alternatively with two different atomic number densities to correct for the frequency shift due to the cold collisions at each measurement campaign. Typical value of the collision shift for 10 or 15 days period is between 8×10^{-15} and 10×10^{-15} and then the associated uncertainty is 1.8×10^{-15} in NICT-CsF1.

C. Microwave Power Dependence Shift

Microwave-related shifts are evaluated by high power

TABLE I. SYSTEMATIC FREQUENCY BIASES AND UNCERTAINTIES

Physical Effect	Bias	Uncertainty
2nd Zeeman	72.5	<0.1
Collision*	-9.0	1.8
Blackbody Radiation	-16.9	0.4
Gravity Potential	8.4	0.1
MW-PW dependence	-0.7	0.3
Cavity Pulling	<0.1	<0.1
Rabi Pulling	<0.1	<0.1
Ramsey Pulling	<0.1	<0.1
Spectral impurities	<0.1	<0.1
Light Shift	<0.1	<0.1
Distributed cavity phase	<0.1	0.3
Majorana	<0.1	<0.1
Background Gas	<0.1	0.3
Total (Type B)		1.9

units are fractional frequency in 10^{-15}

*Typical value

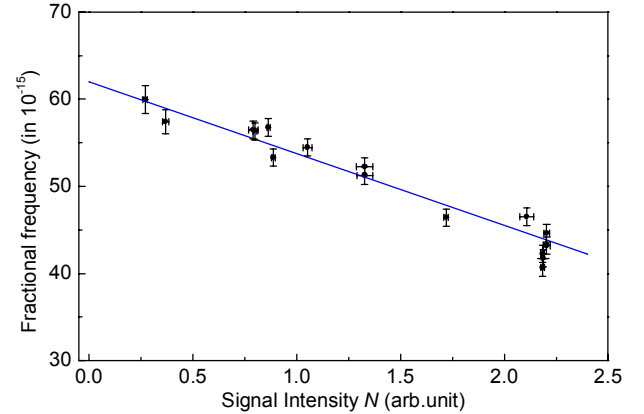


Figure 1. The fractional frequency difference between NICT-CsF1 and the hydrogen maser as a function of the number of detected atoms.

microwave test $b\tau_r$ (changing the microwave field amplitude from $\pi/2$ to $9\pi/2$ (odd multiplies of $\pi/2$)), where b is the Rabi frequency and τ_r is the interaction time in the microwave cavity. An evaluation of the frequency shift associated with the microwave is not simple because many systematic effects, for example, microwave purity, microwave leakage, distributed cavity phase, are convoluted in this shift [6, 7]. It is difficult to separate one from others. It is, however, considered that the microwave power dependent shift is classified into two types as follows;

- a term linearly dependent on the microwave power
- an oscillating term dependent on the microwave amplitude

By investigating the behavior of these two types of shifts, we can evaluate the shift and uncertainty at the normal operation ($b\tau_r = \pi/2$). By high power microwave test, we found the microwave power dependent shift of NICT-CsF1 shown in Fig. 2. By the least square fitting with two contributions, the microwave power dependent shift due to several effects at the amplitude of $\pi/2$ is estimated to be -0.7×10^{-15} with a standard deviation of 0.2×10^{-15} . Considering that the measurement points are not so many, from the aspect of freedom degree of the fitting, we make a modest estimation of an uncertainty of 0.3×10^{-15} .

D. Other Corrected Shift

The room for NICT-CsF1 is well temperature controlled at 297 K (± 0.1 K). NICT-CsF1 is operated at 298 K in equilibrium, and a bias due to the blackbody radiation is estimated to be -16.9×10^{-15} . Considering the thermal gradient and the thermal conductivity, we estimate an uncertainty of 0.4×10^{-15} corresponding to 2 K.

The height of the Ramsey cavity in NICT-CsF1 is measured by a company [8] as 114.7 m in the GRS80 reference flame, which corresponds to 76.6 m above the geoid surface. Here we used Japanese geoid model 'GSIGEO2000'[9, 10]. The gravitational red shift is calculated to be 8.4×10^{-15} . Considering lunar and solar tidal displacement of the Earth's crust, the uncertainty in this shift is below 1×10^{-16} .

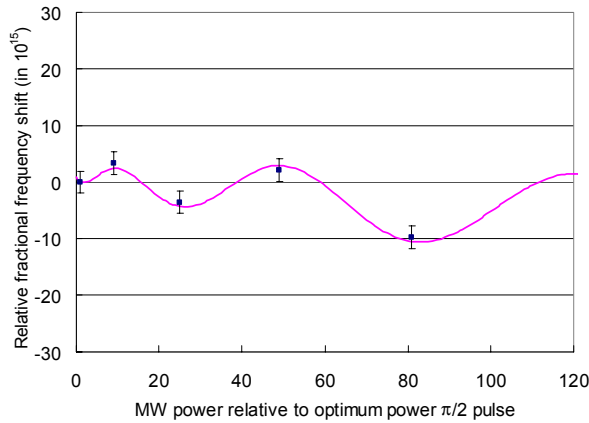


Figure 2. Microwave power dependence shift.

E. Uncorrected Shift

The resonance frequency of the microwave cavity in NICT-CsF1 is closer (700 kHz) to the clock transition. We estimate a bias for the cavity pulling shift is below 1×10^{-16} . From the population difference between the $m_F = 0$ and the $m_F \neq 0$ components, the Rabi pulling shift and the Ramsey pulling shift are calculated to be much less than 1×10^{-16} . The light shift is also negligibly small because all laser beams are blocked by some mechanical shutters during the Ramsey time. From the phase noise of the synthesizer the frequency shift due to the spectral impurity is estimated to be less than 1×10^{-16} . The uncertainty of the frequency shift due to the background gas is estimated to be 3×10^{-16} .

V. FREQUENCY MEASUREMENTS AND REMOTE COMPARISON

The validity of the frequency of NICT-CsF1 was checked by the following frequency comparisons with other primary frequency standards or TAI. Firstly, the frequency difference between NICT-CsF1 and the hydrogen maser HM8 was obtained from the error signal fed back to the synthesizer. Secondly, the frequency difference between HM8 and UTC(NICT) is obtained from time comparison of 1pps signal by a time-interval counter. Thirdly, the frequency difference y_3 between UTC (or TAI) and UTC (NICT) is obtained from the Circular T. Consequently, the frequency difference of NICT-CsF1 with respect to TAI is calculated with combining several uncertainties (Type A and B uncertainties of NICT-CsF1, uncertainty in the link between NICT-CsF1 and UTC (NICT), uncertainty in the link to TAI etc.)

We have operated NICT-CsF1 several times (MJD54014-54029, MJD54029-54039, MJD54039-54049, MJD54079-54094), though the data have not contributed to TAI. During campaigns, NICT-CsF1 was operated at two different atomic number densities in the alternative mode to correct for the collision shift. The transition frequency of ($F = 4$, $m_F = 1$) – ($F = 3$, $m_F = 1$) transition was tracked for 10 minutes everyday to correct for the second Zeeman shift. The other corrected biases were checked before and after the campaign. In these periods, we estimated the Type A uncertainty to be

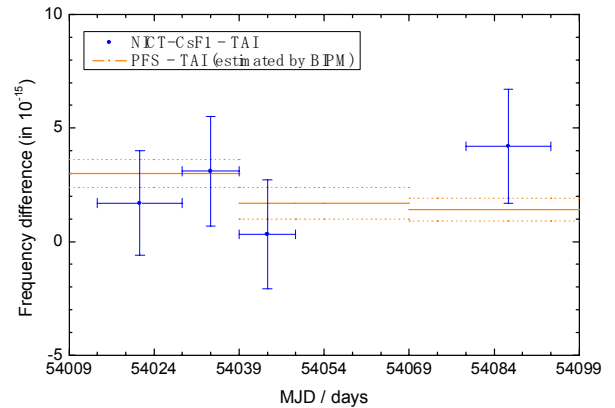


Figure 3. The frequency difference between NICT-CsF1 and TAI during several campaigns

1.4×10^{-15} conservatively considering the frequency stability and the statistic uncertainty of evaluation of frequency shifts. Fig.3 shows the frequency differences between NICT-CsF1 and TAI with the total uncertainty including the uncertainty in the link to TAI. These results were in good agreement with the BIPM estimation of the duration of the TAI scale interval within the stated uncertainties.

During MJD54079-54094 (15 days period), NICT-CsF1 was operated simultaneously with Physikalisch-Technische Bundesanstalt (PTB) fountain clock (PTB-CsF1) [11, 12] for a remote comparison. Each atomic fountain was running related to each hydrogen maser, and the frequency differences between the fountain clock and the hydrogen maser were measured at each institute. The frequency difference between the hydrogen masers at NICT and PTB was measured directly by the Two-Way Satellite Time and Frequency Transfer (TWSTFT) link between NICT and PTB established in 2005 [13]. Combined these frequency differences, NICT-CsF1 and PTB-CsF1 were found to agree with the total uncertainty of 2.9×10^{-15} , which is mainly dominated by the uncertainty of NICT-CsF1 so far. This is the first result of the remote comparison of the primary frequency standards via the long baseline link established between Europe and Asia. The result agreed well with the other comparison methods (GPS-Career Phase, GPS All-in-view and Circular T). Detail discussion will be presented elsewhere [14].

VI. NICT SECOND CAESIUM FOUNTAIN CSF2

NICT-CsF1 has been developed to aim at the stable operation in the level of 10^{-15} . For the purpose, it was designed to be simple and conventional. Toward the operation in the level of 10^{-16} , we have been developing the second caesium atomic fountain NICT-CsF2 with introducing some more techniques. The large point of difference between CsF1 and CsF2 is the laser cooling mechanism. CsF2 adopts (1,1,1) laser cooling geometry to capture the atoms by pure optical molasses. This (1,1,1) geometry enables us to capture many atoms by extending the diameter of the laser cooling beams. And, by capturing in the optical molasses, it is expected to reduce the atomic number density and minify the collisional shift. As another geometrical change, the microwave interaction region is 10cm extended to improve the magnetic inhomogeneity of C-field. On other points, CsF2 has the same structure as CsF1.

Two or more operational atomic fountains in the same level will be a great help for the high level accuracy evaluation. Actually, in the accuracy evaluation of CsF1, the day to day frequency variation of the reference obscured the evaluation of the systematic frequency shifts. As a result, long measurement time was required to remove the influence due to the frequency drift of the hydrogen maser. By comparing multiple atomic fountains operated with relative to the same reference, an evaluation free from the reference instability is possible. It is considered to make the evaluation time shorter and to evaluate of the frequency shifts and their uncertainties more

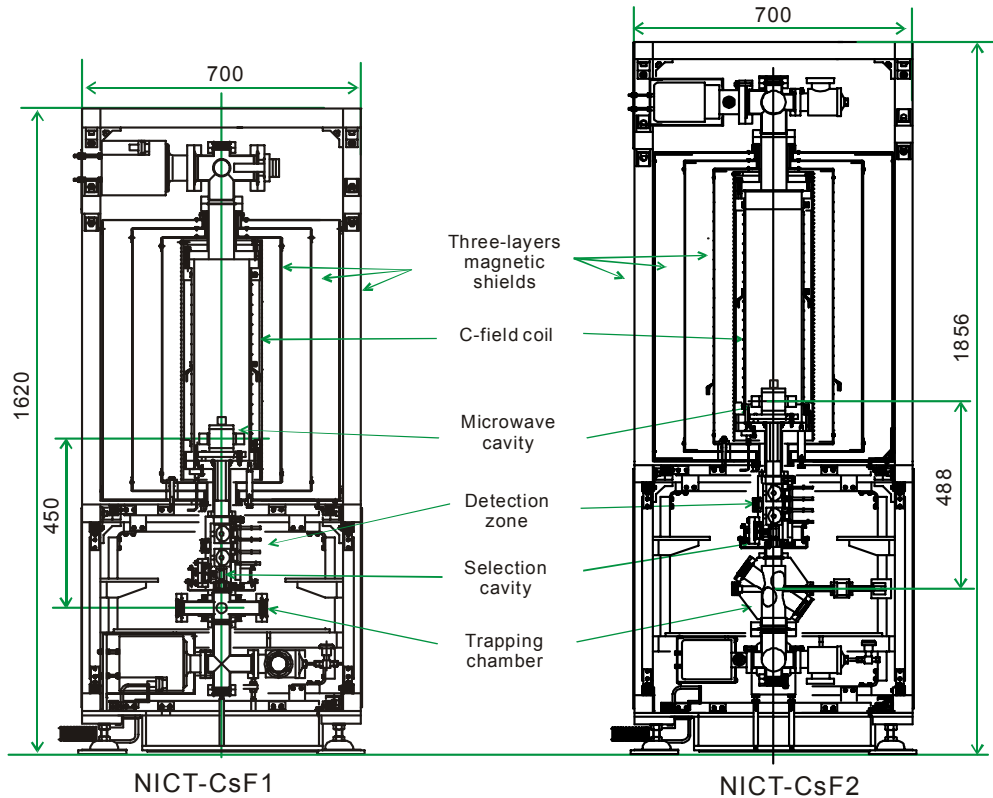


Figure 4. Physical Package Structure of NICT- CsF1 & CsF2.

accurately. This is the expected roll for CsF2.

The vacuum vessel of CsF2 has already been assembled, by using two ion pumps and two NEG pumps, ultra-high vacuum of 2×10^{-8} has been achieved in all regions. The optical setup, adopting the optical fiber modules, will be completed soon. We are planning it to be operational sometime this year.

VII. SUMMARY

NICT have developed the Cs atomic fountain frequency standards NICT-CsF1. In this paper, the basic structure and the accuracy evaluation of NICT-CsF1 was reported. The achieved frequency stability is $4 \times 10^{-13} / \tau^{1/2}$. Several frequency shifts due to the systematic effects have been evaluated. NICT-CsF1 has realized the definition of the SI second with the typical type B frequency uncertainty of 1.9×10^{-15} .

NICT-CsF1 linked to the UTC (NICT) has been operated several times to compare with TAI. The results are in good agreement with the BIPM estimation of the duration of the TAI scale interval. Furthermore, NICT-CsF1 has been directly compared with PTB-CsF1 via the TWSTFT between NICT and PTB. They show good agreement within the uncertainties. It is planned that the comparison data of NICT-CsF1 will be sent to the BIPM to contribute to TAI.

Our second atomic fountain NICT-CsF2 has been developing to confirm the accuracy evaluation more accurately. It will be operational soon and will be compared with CsF1.

ACKNOWLEDGMENT

The authors wish to acknowledge the technical helps of S. Weyers, R. Wynands, M. Fujieda, D. Piester and A. Bauch on the remote comparison via the TWSTFT.

REFERENCES

- [1] Y. Hanado et al, "The New Generation System of JAPAN Standard Time at NICT" *Proc. Asia-Pacific Workshop on Time and Frequency*, 69-76, 2006
- [2] M. Kumagai, H. Ito, M. Kajita, and M. Hosokawa, "New cesium atomic fountain frequency standard at NICT", *Proc. 19th Euro. Freq. Time Forum*, 278, 2005
- [3] M. Kumagai, H. Ito, M. Kajita, and M. Hosokawa, "NICT's operational atomic fountain NICT-CsF1", *Proc. 2006 Asia-Pacific Workshop on Time and Frequency*, 77-83, 2006
- [4] M. Kumagai, H. Ito, M. Kajita, and M. Hosokawa, "Recent progress on Cs atomic fountain at NICT", *Proc. 18th Euro. Freq. Time Forum*, 2004
- [5] <http://www.spectrodynamics.com/>
- [6] S. Jefferts, J. Shirley, N. Ashby, E. Burt, G. Dick, "Power dependence of distributed cavity phase-induced frequency biases in atomic fountain frequency standards" *IEEE Trans. Ultrason. Ferroelect. Freq. Contr.* 12 2314-2321, 2005

- [7] S. Weyers, R. Schröder, R. Wynands, "Effect of microwave leakage in Caesium clocks: theoretical and experimental results", *Proc. 20th Euro. Freq. Time Forum*, 173-180, 2006
- [8] <http://www.kkc.co.jp/english/>
- [9] H. Nakagawa et al, "Development of a New Japanese Geoid Model, "GSIGEO2000", *Bulletin of the Geographical Survey Institute* 49, 1, 2003
- [10] Y. Kuroishi, H. Ando, Y. Fukuda, "A new hybrid geoid model for Japan, GSIGEO2000", *Jour. Geodesy* 76, 428-426, 2002
- [11] S. Weyers, U. Hubner, B. Fischer, R. Schröder, Chr. Tamm, and A. Bauch, "Uncertainty evaluation of the atomic caesium fountain CSF1 of the PTB", *Metrologia* 38, 343-352, 2001
- [12] S. Weyers, A. Bauch, R. Schröder, and Chr. Tamm, "The atomic caesium fountain CSF1 of PTB", *Proc. 6th Symposium on Frequency Standards and Metrology* (World Scientific), 64-71 (2002)
- [13] M. Fujieda et al, "Long baseline TWSTFT between Asia and Europe" *2006 Proc. Precise Time and Time Interval*, in press
- [14] M. Fujieda et al, "First comparison of primary frequency standards between Europe and Asia", *Proc. EFTF-IEEE-FCS2007*, unpublished